

Supplementary Information

Plug-and-play safe-by-design production of metal-doped tellerium nanoparticles with safer antimicrobial activities

*Dae Hoon Park,^{‡a} Milan Guatam,^{‡b} Sung Jae Park,^a Jungho Hwang,^{*a} Chul Soon Yong,^b Jong Oh Kim^{*b}
and Jeong Hoon Byeon^{*c}*

^aSchool of Mechanical Engineering, Yonsei University, Seoul 03722, Republic of Korea

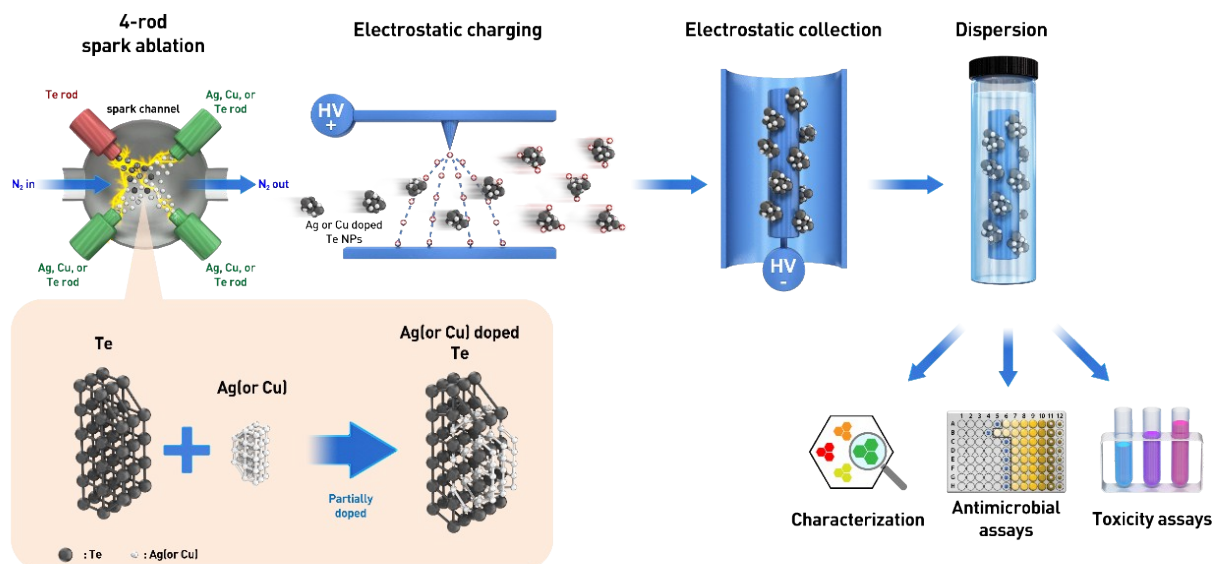
^bCollege of Pharmacy, Yeungnam University, Gyeongsan 38541, Republic of Korea

^cSchool of Mechanical Engineering, Yeungnam University, Gyeongsan 38541, Republic of Korea

[‡]These authors contributed equally to this work.

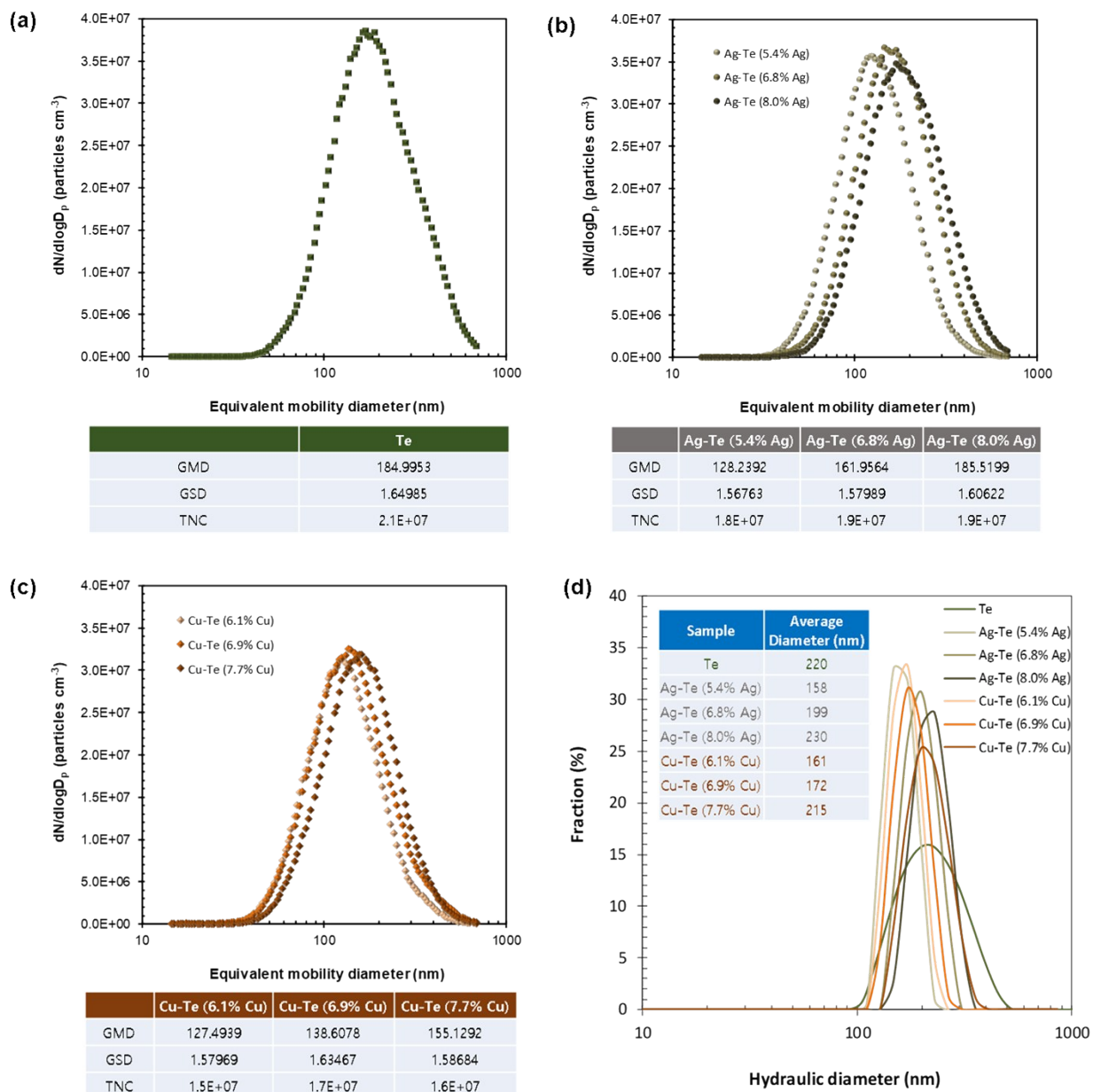
^{*}Corresponding authors: postjb@yu.ac.kr, jongohkim@yu.ac.kr, and hwangjh@yonsei.ac.kr

FIG. S1



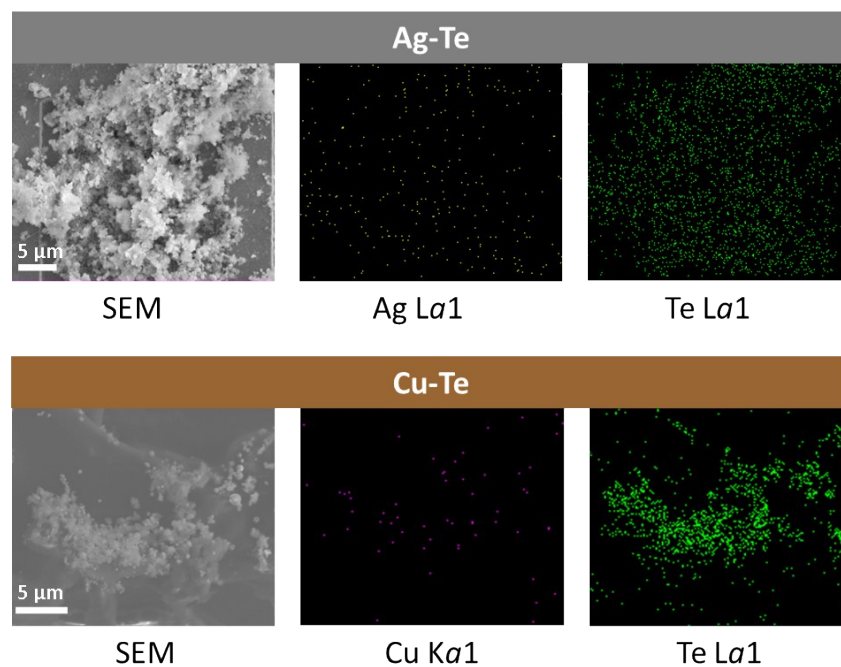
Schematic of the plug-and-play continuous flow protocol for the production of Ag- or Cu-doped Te nanoparticles. The compact (8 cm^3) spark chamber comprised three Ag or Cu anodes and a Te cathode, and parts of the electrodes were evaporated using an AC power supply. Vapors were subsequently condensed to form Ag–Te or Cu–Te particles over a temperature gradient, and atomic Ag or Cu were incorporated into base Te structures at precisely 5%–8% by varying the numbers of operating Ag or Cu electrodes (1–3). The AC electric field with high frequency (2.5 kHz) was used to accelerate Ag or Cu incorporation into base Te matrixes, and Ag_2Te or Cu_2Te were generated following bipolar charging of the vapors. To confirm antimicrobial activities and biocompatibility, Ag–Te or Cu–Te particles were dispersed in buffered saline and were then collected by dipping an electrostatically charged collection rod into the solution with bath sonication. The results of antimicrobial and toxicity assays were used to estimate SI values of the particles.

FIG. S2



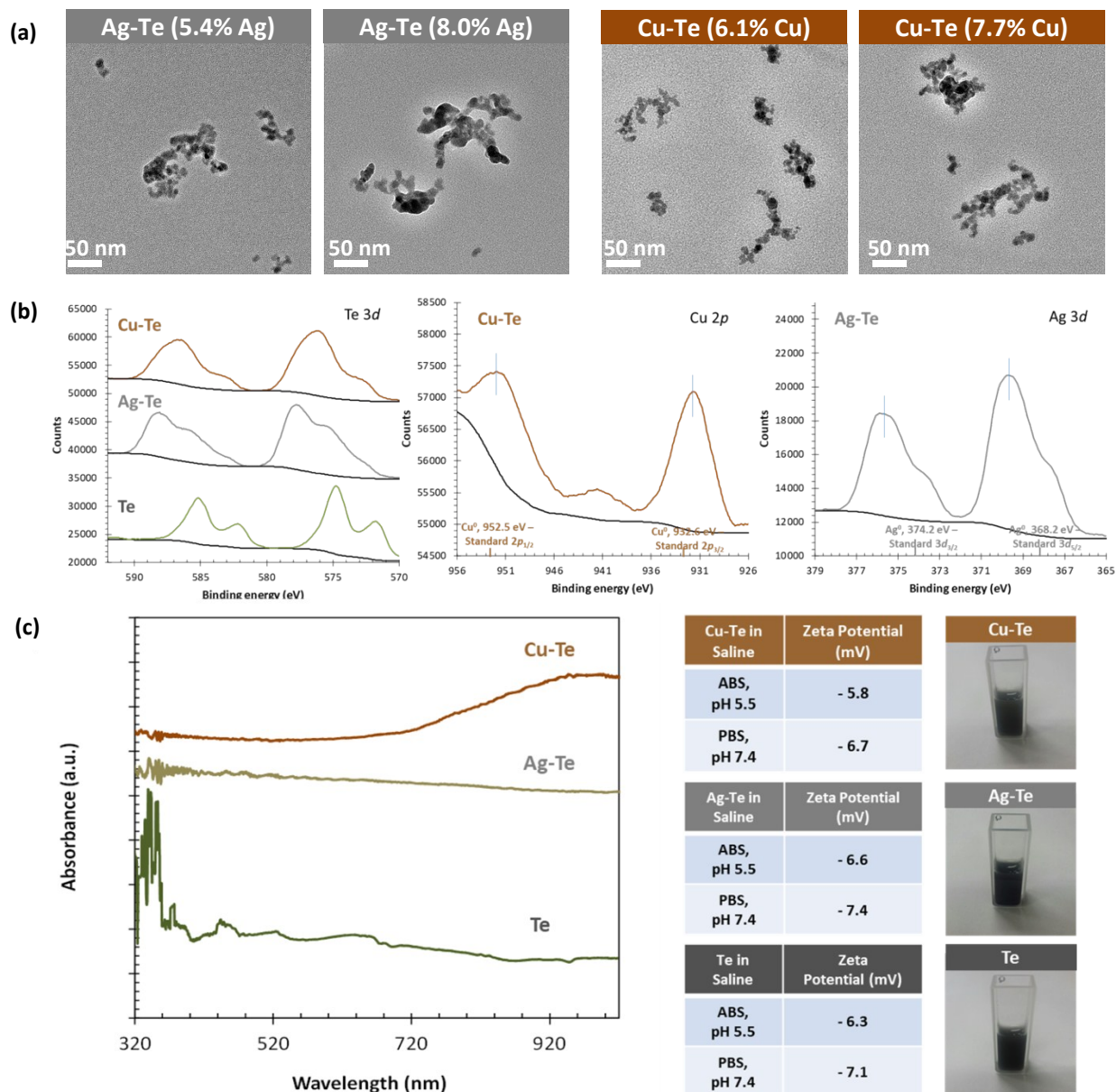
Size distributions of Ag–Te and Cu–Te particles suspended in gaseous (a-c) and aqueous (d) media; differences in particle concentrations induced discrepancies of sizes between GMD (gaseous) and average diameters (aqueous). The significantly larger concentration for DLS measurements than for SMPS induced mismatches due to agglomeration or scattering errors.

FIG. S3



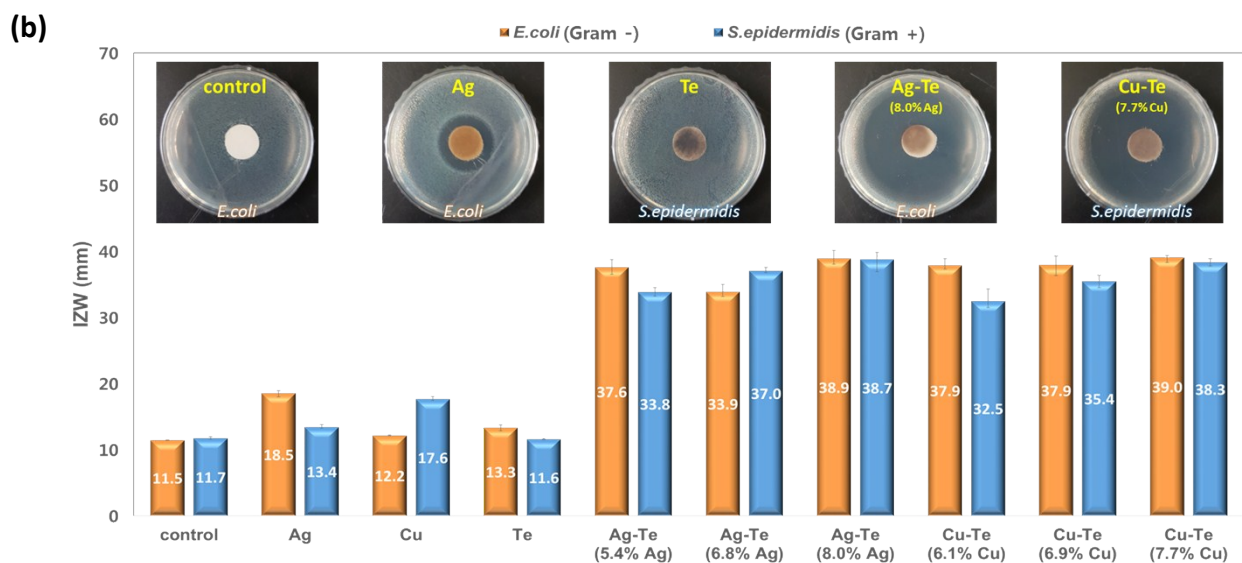
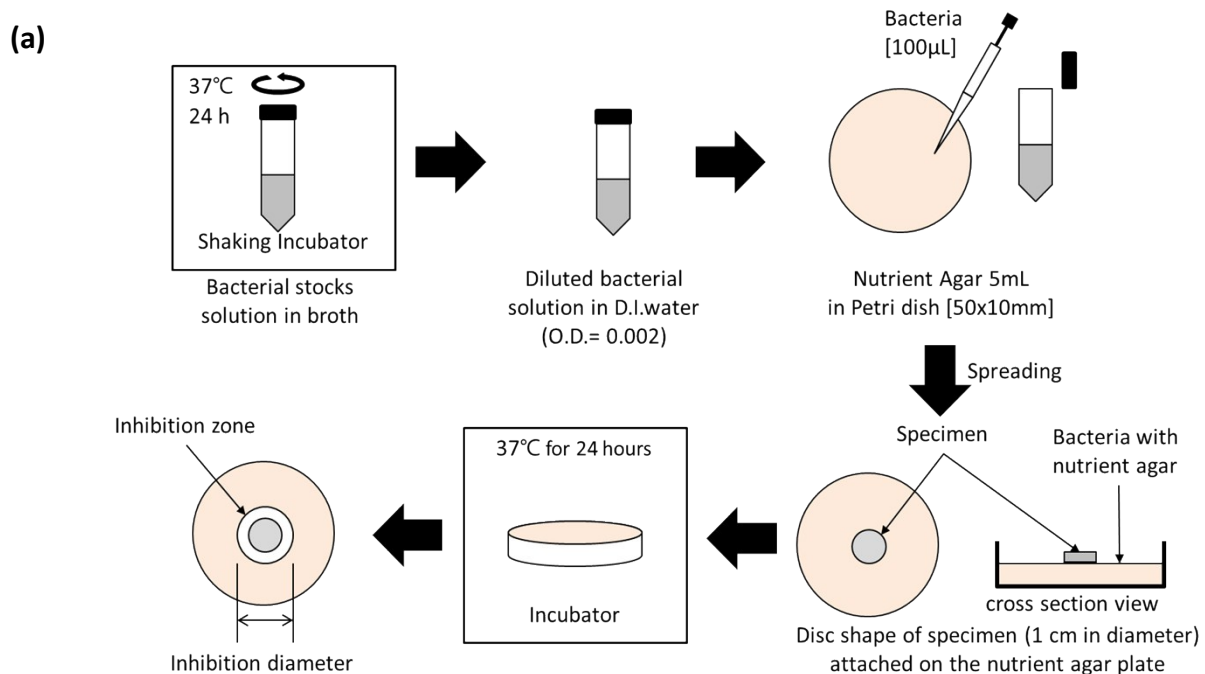
Elemental analyses of Ag–Te and Cu-Te particles that were generated with 2 Ag or Cu anodes. Ag or Cu contents and distributions of particles were determined using EDX mapping. Ag or Cu contents in particles were further confirmed in comparison with XPS analyses.

FIG. S4



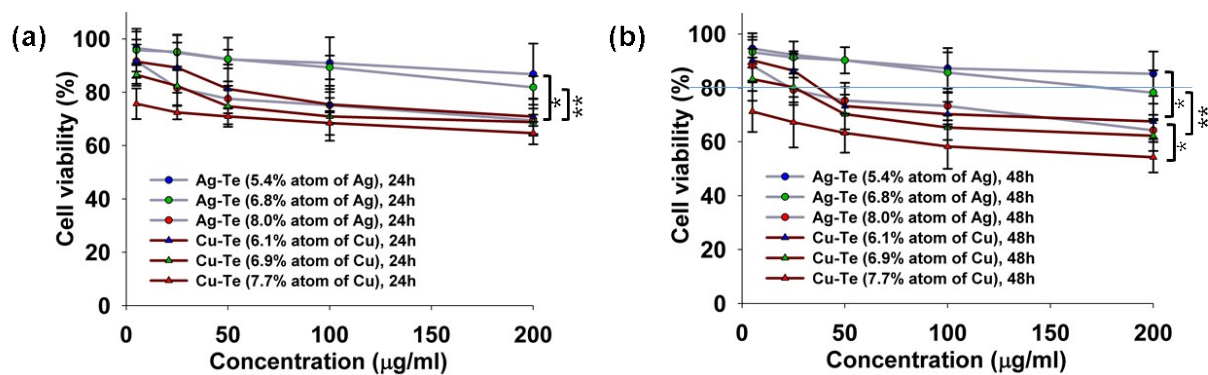
(a) TEM images of Ag–Te (5.4% and 8.0% Ag) and Cu–Te (6.1% and 7.7% Cu) particles. Microstructures and light absorption properties of particles that were produced using 2 Ag or Cu anodes; (b) Te3d, Cu2p, and Ag3d core XPS spectra of Ag–Te and Cu–Te particles; band shifts from Ag or Cu-doping were verified by comparing nanoparticles of Te, Ag, and Cu. (c) UV-vis spectra and zeta potentials of Ag–Te and Cu–Te dispersions were compared with those of Te particles. Inset digital images are of dispersions.

FIG. S5



Disc diffusion antimicrobial assay. (a) Schematic of disc diffusion method employed in this study. To examine IZW, the particles were deposited on disc substrates being attached to growth medium plate. (b) IZW results from the disc diffusion method. Digital images of the representative cases are shown as insets.

FIG. S6



Cytotoxicities of Ag-Te and Cu-Te particles after 24- (a) and 48-h (b) incubations with HDF cells at particle concentrations of 5–200 $\mu\text{g mL}^{-1}$; $p < 0.05$, $**p < 0.01$. Concentrations that reduced cell viability to $>90\%$ were used to estimate SI.